Nitrogen Cycling Driven By Organic Matter Export In The South Pacific Oxygen Minimum Zone

T. Kalvelage, G. Lavik, P. Lam, Sylvie Contreras, L. Arteaga, C. R. Loscher, A. Oschlies, A. Paulmier, L. Stramma, M. M. M. Kuypers

Nitrogen cycling driven by organic matter export in the South Pacific oxygen minimum zone

Tim Kalvelage[1], Gaute Lavik[1], Phyllis Lam[1], Sergio Contreras[1,4], Lionel Arteaga[2], Caroline Löscher[3], Andreas Oschlies[2], Aurélien Paulmier[1,5,6], Lothar Stramma[2], Marcel M.M. Kuypers[1]

[1]Max Planck Institute for Marine Microbiology, Bremen, Germany
[2]GEOMAR Helmholtz Centre for Ocean Research Kiel, Germany
[3]Institute for General Microbiology, Kiel, Germany
[4]Current address: Large Lakes Observatory, University of Minnesota Duluth, USA
[5]Current address: Laboratoire d'Etudes en Géophysique et Océanographie Spatiales, Toulouse, France
[6]Current address: Instituto del Mar del Perú (IMARPE), Esquina Gamarra y General Valle S/N Chucuito Callao, Peru

Keywords: marine nitrogen cycle, export production, organic matter, nitrogen loss, N-deficit, anammox, secondary nitrite maximum, oxygen minimum zone, eastern tropical South Pacific, Peruvian upwelling system

Oxygen minimum zones are major sites of oceanic nitrogen-loss, and have been expanding globally. Nitrogen-loss occurs mainly as the production of dinitrogen gas by denitrification or the so-called anammox process – the anaerobic ammonium oxidation with nitrite. Activity of anammox has been found more common in recent studies in the eastern tropical South Pacific, one of the largest oxygen minimum zones worldwide. As anammox requires substrates from multiple co-occurring nitrogen transformations, regulation of nitrogen-loss has to involve factors controlling overall nitrogen cycling, but which exactly remains unclear. Here, we present the most comprehensive nitrogen budget assessment for all major nitrogen fluxes to date for the eastern tropical South Pacific oxygen minimum zone. Extensive ^{15}N-labelling experiments, nutrient measurements and export production modelling, together show that overall nitrogen cycling therein are tightly linked to the export of organic matter. Nitrogen-loss is most active over the productive shelf, fuelled by high rates of sinking organic matter and benthic ammonium release; then declines sharply offshore. These results highlight the importance of coastal oxygen minimum zones in oceanic nitrogen balance, and offer an empirical relationship for parameterization in biogeochemical models to more realistically assess the effects of climate change on oceanic carbon and nitrogen cycling.

Coastal upwelling of nutrient-rich deep water fuels high surface productivity at the eastern boundaries of (sub)tropical oceans. The resultant export of organic matter stimulates strong microbial respiration in the subsurface. Combined with poor ventilation, permanently O_2-deficient waters called oxygen minimum zones (OMZs) develop at mid-depths[1,2]. Ongoing, global expansion and intensification of OMZs will expectedly continue as anthropogenic pressures on marine environments grow[3,4,5].

Although constituting only ~1% ($O_2 \leq 20$ µmol kg^{-1}) of global ocean volume[6], OMZs have a profound impact on oceanic nitrogen (N) balance as they account for ~20-40% of global oceanic N-loss[7]. Ocean de-oxygenation might enlarge the ocean volume subject to N-loss[8], exacerbate N-limitation of phytoplankton, and reduce the ocean's capacity to attenuate rising atmospheric carbon dioxide. Assessing the effects of expanding OMZs on the future ocean's nutrient balance, however, remains speculative, as biogeochemical models do not reproduce present-day global patterns of N-loss[9,10,11]. A major deficiency of those models appears to be the poor representation of coastal regions; whereas an increasing number of studies indicates that N-loss in shelf OMZs[12,13,14], coastal-offshore OMZ water mass exchange[15] and OMZ-sediment interactions[16] play more important roles on the overall N-budget.

Based on the observed accumulations of nitrite (NO_2^-) and associated N-deficits, most N-loss in OMZ waters has traditionally been attributed to heterotrophic denitrification[17,18,19], the stepwise reduction of nitrate (NO_3^-) to gaseous dinitrogen (N_2). Recent studies have, however, often failed to detect significant denitrifying activity in OMZs; rather, anammox has more commonly been identified as a major N_2-forming pathway in these environments[12,13,14,20].

The regulation of N-loss activity including anammox is not fully understood. Anammox requires NH_4^+ and NO_2^-. Sources and sinks of both compounds have been identified in the OMZs, including aerobic NH_3 and NO_2^- oxidation, as well as anaerobic NO_3^- reduction to NO_2^- and dissimilatory NO_3^-/ NO_2^- reduction to NH_4^+ (DNRA)[14,15,21,22]. Surprisingly, O_2 sensitivity assays show that these processes in OMZ waters share a large overlapping range of O_2 concentrations (>0-20 µmol L^{-1}) in which they can co-occur, implying that within this range, controlling factors other than O_2 are more important[23,24]. Enhanced autotrophic and heterotrophic N-cycling activity in the upper OMZ[13,14,20,21], and

generally elevated anammox rates usually measured in coastal versus offshore OMZs[6], suggest that N-loss might ultimately be regulated by export production of organic matter.

To test this hypothesis, we conducted a large-scale survey of N-cycling rates, functional gene abundances, chlorophyll, nutrient and O_2 concentrations, as well as modelled export production, throughout the eastern tropical South Pacific (ETSP), one of the three major OMZs in the world.

Dissolved Inorganic Nitrogen in the South Pacific Oxygen Minimum Zone

Consistent with past observations in the ETSP[18,26], pronounced secondary NO_2^- maxima were found in the offshore OMZ between 10°S and 18°S (supplementary Fig. 1), extending up to 100's km westward with maximum concentrations of ~11 μmol L^{-1}. Based on the spatial distribution of measured O_2, the lower OMZ boundary occurred at ~600 m on average near the Peruvian shelf (Figs S1-2). Henceforth, this is used as a depth cut-off to differentiate coastal OMZ stations, where the OMZ is in direct contact with sediments and benthic N-fluxes (<600m), from all others that are defined as offshore OMZ stations. Integrated over the thickness of the OMZ (defined by $O_2 \leq 15$ μmol L^{-1} where N-loss activity remains detectable in O_2-sensitivity assays[24]; Figs 1b, S2), NO_2^- concentrations reached >2 mol m^{-2} in the offshore region (Fig. 1d). Concentrations of NH_4^+ were low (<0.25 μmol L^{-1}) throughout the OMZ, but could be ≥0.5 μmol L^{-1} over the shelf and near the upper OMZ boundary further offshore. Deeper in the offshore OMZ, plumes of elevated NH_4^+ concentrations (≤~3 μmol L^{-1}) sometimes occurred (supplementary Fig. 1), resulting in high depth-integrated values (Fig. 1e).

Offshore OMZs were characterized by severe N-deficits, expressed here as strongly negative N* with minima from -8 μmol N L^{-1} at 3.58°S down to -32 μmol N L^{-1} at 16°S. Depth-integrated values of N* (Fig. 1e) and NO_2^- were significantly correlated (Spearman

R=-0.61, $p \leq 0.001$). The southward intensification of both NO_2^- maxima and N* minima likely reflects the accumulated effects of time-integrated microbial activity in OMZ waters that advect poleward along the continental slope with the Peru-Chile Undercurrent [27,28]. Over the Peruvian shelf between 12°S and 14°S, extreme N-deficits (N* down to -60 μmol L^{-1}, Supplementary Fig. 1) were detected along with the presence of hydrogen sulphide (H_2S). These stations are not further considered in the remaining discussions unless otherwise indicated, as the resident microbial communities and processes profoundly differ from typical OMZ scenarios (Schunck et al. submitted.).

Sources of Nitrite

Nitrite in the OMZs can be generated by NH_3 oxidation, the first step of nitrification; or by the reduction of nitrate to nitrite[6,21,22]. Ammonia oxidation has been identified as an important NO_2^- source in the Peruvian OMZ, that is active under near-anoxic conditions[21,23,29]. Our measured rates of NH_3 oxidation generally peaked at the base of the oxycline (~90 nmol N L^{-1} d^{-1}), decreased to detection limit at the stations furthest offshore, and were not detectable in the core of the OMZ (Tables 1 and S2). The presence of both archaeal and bacterial ammonia-oxidizers is verified by the detection of their biomarker functional genes encoding ammonia monooxygenase subunit A (Tables 1 and S3).

Integrated over the thickness of the OMZ, NO_2^- production via NH_3 oxidation increased from undetectable at the westernmost stations to ≤4.7 mmol NO_2^- m^{-2} d^{-1} near the coast (Fig. 2a; supplementary Table 1). For the entire OMZ volume examined (~5.5×10^5 km^3), NH_3 oxidation is estimated to produce ~3.8 Tg N y^{-1} of NO_2^-, with 24% attributed to coastal OMZ (≤600 m) and 76% offshore (>600 m) (Fig. 3). Although significant rates have also been reported for the surface mixed layer in the ETSP[30], the mixed layer was not included in the current OMZ budget.

Overall, NH_3 oxidation accounted for only ~7% of the total NO_2^- production. The majority came from NO_3^- reduction to NO_2^-, consistent with previous findings in the Peruvian, Namibian and Arabian Sea OMZs[15,21,22]. Apart from its association with anammox, NO_3^- reduction to NO_2^- is the first step in denitrification and DNRA, and NO_3^- is the next preferred terminal electron acceptor after O_2 for the oxidation of organic matter. NO_3^- reduction was detected throughout the OMZ at all investigated stations; it reached a maximum (~1 μmol N L^{-1} d^{-1}) over the central shelf, but dropped to ~10 nmol N L^{-1} d^{-1} at the westernmost offshore stations (Table 1).

Depth-integrated rates showed similarly declining trend offshore (Fig. 2c; supplementary Table 1). Integration over the whole region yields an annual NO_3^- reduction of ~49 Tg N, of which 29% occurs in the coastal OMZ and 71% offshore (Fig. 3). Like previous observations from the Peruvian[23] and the Arabian Sea[15] OMZs, NO_3^- reduction significantly correlated with depth-integrated NO_2^- concentrations (Spearman R=0.71, $p \leq 0.001$) (Table 2), which indicates that NO_3^- reduction is a major contributor to the secondary NO_2^- maxima.

Sinks of Nitrite

Nitrite oxidation, the second step in nitrification, was most active in the upper OMZ throughout the ETSP. Its activity was detected deeper into the OMZ than NH_3 oxidation, consistent with earlier reports[23,29]. Nitrite oxidation rates were highest (928 nmol N L^{-1} d^{-1}) over the Peruvian shelf despite low O_2 levels (Table 1), and declined sharply to ≤~20 nmol N L^{-1} d^{-1} along the furthest offshore transect. Although NO_2^- oxidation is believed to require O_2, this process has been detected at <1-2 μmol O_2 L^{-1} in the Peruvian[23,29] and Namibian OMZs[22]. O_2 sensitivity assays (~1-25 μmol L^{-1}) at two stations further demonstrated only a moderate attenuation by low O_2 (at most ~50% activity reduction at <1 μmol L^{-1})

(supplementary Fig. 3), which agrees well with observations in the Namibian OMZ[22]. Clearly, NO_2^- oxidizers are well adapted to O_2-deficient environments.

NO_2^--supply from NH_3 oxidation, the first step of nitrification, is thought to constrain NO_2^- oxidation rates. Despite the significant correlation between NH_3 and NO_2^- oxidation rates (Spearman R=0.73, $p \leq 0.001$) (Table 2), NO_2^- oxidation in the ETSP OMZ exceeded those of NH_3 oxidation often by more than tenfold (Fig. 2a,b; supplementary Table 1,2). Similar observations in the OMZs off Namibia[22] and Peru[23,29], indicate a decoupling of the two steps of nitrification in O_2-deficient systems. A likely alternative NO_2^- source is NO_3^- reduction.

Based on modeled N-fluxes a NO_2^- "shunt", in which 45-74% of the NO_3^- reduced to NO_2^- by "denitrifying" micro-organisms is re-oxidized by aerobic NO_2^- oxidizers, has been proposed for the ETSP[31]. In agreement, our annual rates of NO_2^- oxidation for the coastal (7 Tg N y^{-1}) and offshore OMZ (23 Tg N y^{-1}) are equivalent to 51% and 65%, respectively, of NO_3^- reduction (Fig. 3). The strong correlation between the two processes (Spearman R=0.75, $p \leq 0.001$) (Table 2) indicates a close coupling between NO_2^- oxidation and NO_3^- reduction in the ETSP OMZ.

Meanwhile, only sporadic and low rates of DNRA ($\leq$1.3 nmol L^{-1} d^{-1}) were detected during our sampling period (Table 1). A general lack of detectable *nrfA*, a key functional gene encoding for the cytochrome *c* NO_2^- reductase corroborates these results (Table 1). DNRA appears to exhibit a high degree of spatio-temporal variability, with similarly low rates measured on the Namibian shelf[22], but with tenfold greater rates and *nrfA* gene abundance than observed in the OMZs off Peru[21] and Oman[14]. Hence, we cannot exclude DNRA as a significant NO_x^--sink for and NH_4^+-source in the ETSP at other times.

Nitrogen-Loss Activities

At the time of our sampling, denitrification, expressed as the production of $^{30}N_2$ from $^{15}NO_x$, was generally non-detectable. Low rates of denitrification (~2-5 nmol L^{-1} d^{-1}) were measured in three samples from the Peruvian shelf OMZ (Tables 1, S2). Substantially higher rates were detected in few samples containing measurable amounts of H_2S (Fig. 2e; supplementary Tables 1,2), suggesting a coupling with H_2S oxidation (ref. 32; Schunck et al. submitted.). In contrast to the conclusion drawn by a recent study[33], water-column denitification was only of minor importance (<<1% total N-loss) for the overall N-budget in the ETSP OMZ (supplementary information).

N_2 production attributed to anammox was detected at all stations except the two furthest offshore, consistentent with previous studies in the ETSP[13,20,34],. Anammox activity was often enhanced in the upper OMZ and markedly elevated in the bottom waters over the shelf and upper continental slope. Rates were highest (≤~225 nmol N L^{-1} d^{-1}) over the central shelf (10°S-16°S) and declined by two orders of magnitude westward (Table 1). The presence of anammox bacteria was verified by the detection of their characteristic hydrazine (N_2H_4) oxidoreductase genes (*hzo1* and *2*) throughout the OMZ; whereas denitrifier-*nirS*, encoding for the cytochrome cd_1-containing NO_2^- reductase, was generally not detectable (Tables 2, S3).

Depth-integrated anammox rates were >10 mmol N m^{-2} d^{-1} on the central shelf, similar to previous findings[13], and <1 mmol N m^{-2} d^{-1} at the furthest offshore stations (Fig. 2d; supplementary Table 1). Altogether, anammox accounts for an annual N-loss of ~10 Tg in an area of $1.2x10^6$ km², which is at the lower end of earlier estimates for the ETSP (9-26 Tg N y^{-1})[13,18,23,35].

Flux measurements of dissolved inorganic nitrogen and N_2 made just prior to our sampling demonstrate that the sediments underlying the OMZ are additional sites of N-loss[16]. Combined with reaction-diffusion modeling, anammox and denitrification were shown to be

active N-sinks in the Peruvian coastal sediments. Based on the reported sedimentary NO_x^- fluxes and NO_x^- partitioning between anammox, denitrification, and DNRA[16], we estimate a loss of 1 Tg N y^{-1} from sediments in contact with the OMZ bottom waters (Fig. 3).

Conventionally, the accumulation of NO_2^- in OMZ waters has been interpreted as signs of active N-loss, and thus, is targeted by most field-sampling campaigns[17,18,19,20,23,26,29]. Our data contradict this interpretation. Unlike NO_2^-, depth-integrated anammox rates did not reveal any meridional trends, but decreased from shelf to offshore. Depth-integrated anammox rates and NO_2^- concentration were only moderately correlated (Spearman R=0.64, $p<0.001$) (Table 2). Furthermore, significant correlations between volumetric rates and NO_2^- concentrations were only observed for the shelf OMZ (Spearman R=0.72, $p<0.001$) and not offshore (Spearman, $p>0.5$). NO_2^- accumulation offshore probably resulted from a greater persistence of NO_3^- reduction to NO_2^- compared to other NO_2^--consuming processes in a poorly ventilated region, where the net NO_2^- gain was about five times higher compared to the coastal OMZ (11.4 and 2.2 Tg N y^{-1}, respectively).

Ongoing water column N-loss cannot be deduced simply from the intensity of N* minima, as shown by the lack of significant correlation (Spearman $p>0.05$) between anammox activity and N* (Table 2). While the depth-integrated N-deficit is strongest (most negative N*) offshore, anammox activity is highest over the shelf and upper continental slope. Though comprising only 10% of the area covered and merely 4% of the sampled OMZ volume, coastal OMZ waters contribute as much as 30% of the total N-loss (Fig. 3). Meanwhile, N-deficits in coastal OMZ waters amount to only 5% (4 Tg N) of the total N-deficit (71 Tg N). Hence, the large N-deficit offshore most likely results from horizontal advection of N-deficient shelf waters[21] that accumulate due to a long residence time in the offshore OMZ (~10 y based on N* and measured N-loss). This is analogous to to recent observations made in the Arabian Sea: substantial NO_2^- accumulation and low N-loss activity

in the central basin, compared to the rapid N-loss over the adjacent productive Omani shelf[14,15].

Sources of Ammonium

N-loss driven by anammox requires NH_4^+, which usually does not accumulate in OMZs. Ammonium concentrations can be kept low by a tight coupling between NH_4^+ production and consumption processes, while the NH_4^+ released at the reported remineralization rates may already be sufficient to fuel anammox. Major sources of NH_4^+ are water-column organic matter remineralization and sedimentary NH_4^+ release.

DNRA and organic matter ammonification are active benthic NH_4^+ sources off the coast of Peru. During two preceding cruises (M77-1 and 2) to the ETSP[16], large NH_4^+ fluxes (~0.5-4 mmol m^2 d^{-1}) from sediments into the overlying OMZ waters were measured on a cross-shelf transect at 11°S. The often enhanced anammox activity in the coastal OMZ bottom waters suggests a strong influence from NH_4^+ diffusing out of the sediments[13,36]. Assuming an average benthic NH_4^+ flux of ~2 mmol m^{-2} d^{-1} and a typical anammox rate of ~4 mmol NH_4^+ m^{-2} d^{-1} for the Peruvian coastal waters, the underlying sediments could supply ~50% of the NH_4^+ needed for the anammox rates observed. Clearly, additional NH_4^+ sources are necessary to fulfil the remaining requirements for anammox, especially in offshore OMZ waters, which are spatially decoupled from the sediments.

Based on the measured NO_3^- reduction rates, subsequent ammonification of Redfieldian organic matter generates 65% and 73% of the NH_4^+ needed for anammox in the coastal and offshore OMZs, respectively (Fig. 3). These are likely underestimates, considering the observed preferential N-degradation of organic matter via NO_3^- respiration under suboxic conditions[37]. Whether the reduction of NO_3^- is directly coupled to the

oxidation of organic matter, or indirectly via a recently proposed cryptic sulphur cycle[38], could not be discerned at this point.

Remineralization of sinking organic matter and subsequent NH_4^+ release is usually enhanced near the upper OMZ boundary, and would support the high anammox and NH_3 oxidation activity observed[13,14,15,20,21,23]. On average, ~40% of their combined NH_4^+ demands are supplied by NO_3^- reduction, with the remainder possibly coming from microaerobic organic matter remineralization[20]. The activity of O_2-dependent nitrification at non-detectable O_2 concentrations in OMZs indicates that microaerobic respiration proceeds even at nanomolar O_2 levels, in accordance with an apparent half-saturation coefficient of <20 nmol L^{-1} previously reported for microaerobic respiration in these waters[39]. High O_2 consumption rates, mainly attributable to heterotrophic respiration, and genes encoding for terminal respiratory oxidases with high O_2-affinities were detected in the ETSP on the same expedition (Kalvelage et al. unpubl.). While there are suggestions that O_2 is efficiently depleted down to the limits of microaerobic respiration in the OMZ core[40], regular intrusions of more oxygenated surface waters or mixing events, such as those related to eddies[41], may sustain aerobic microbial activity in the upper OMZ.

Linking Surface Productivity and Sub-surface Nitrogen Cycling

Depth-integrated anammox rates correlated strikingly well with NO_3^- reduction, NO_2^- oxidation and NH_3 oxidation (Spearman R=0.88, 0.86 and 0.75, respectively; $p \leq 0.001$), indicating a common controlling factor for their concerted activity. Our data suggest that N-cycling processes in the OMZ are tightly coupled to the export of organic matter.

Export of organic matter at the base of the euphotic zone was estimated from net primary production (NPP)[42] and the ratio of export-to-total primary production (*ef*-ratio)[43]. At the time of sampling, NPP was up to ~3 g organic C (C_{org}) m^{-2} d^{-1} near the coast and

decreased to <0.5 g C_{org} m^{-2} d^{-1} further offshore, values typical for the Peruvian upwelling system[44]. Computed *ef*-ratios ranged from 0.16 (low-NPP sites) to 0.42 (high-NPP sites). The resulting N-export production rates (converted from measured C:N=7.2 of surface particulate organic matter) were >10 mmol organic N (N_{org}) m^{-2} d^{-1} over the shelf and in the order of ~1 mmol N_{org} m^{-2} d^{-1} at the stations furthest offshore (Fig. 2f; supplementary Table 1). Export production was highly correlated to depth-integrated rates of anammox, NO_3^- reduction and NO_2^- oxidation (Spearman R=0.79, 0.75 and 0.60, respectively, $p \leq 0.001$) as well as NH_3 oxidation (Spearman R=0.56, $p \leq 0.01$) (Table 2). This suggests that the lateral distribution of N-cycling activity, including anammox, is mainly determined by the export of organic matter, which is the ultimate source of the required reactive substrates NH_4^+ and NO_2^- in the OMZ.

Overall, we estimate NPP of 12 and 47 Tg N y^{-1} in the coastal and offshore surface waters, respectively, which appear reasonable at a net lateral supply of 88 Tg NO_3^- y^{-1} to the upwelling region (Fig. 3). The corresponding export fluxes are 4.4 and 9.9 Tg N_{org} y^{-1}. Taking organic matter sedimentation and export to the deep ocean into account, our results show that the export production to the OMZ is sufficient as an N-source to support the measured N-fluxes.

In summary, extensive sampling and experimentation throughout the ETSP OMZ shows that the activity of anammox and N-linked processes is highly correlated with export production. High productivity over the shelf and upper slope, as well as sedimentary NH_4^+ release, drive high rates of tightly coupled N-cycling processes and thus N-loss via anammox in the shallow coastal OMZ compared to the offshore OMZ.

While the globally expanding OMZs might increase the oceanic volume conducive to N-loss, N-loss would only continue to rise as long as there is sufficient nutrient supply for primary production in the euphotic zone, and nutrient supply is not hampered by intensified stratification (i.e. reduced upwelling) due to ocean warming. These positive and negative

feedbacks are important considerations for biogeochemical models, which at present do not adequately reproduce the observed spatial patterns of N-loss in OMZs. In light of our results, the activities of N-loss via anammox appear to be directly linked to export production rates in biogeochemical models using the following empirical relationship: anammox = 0.7 x N_{org} export (supplementary Fig. 4). This may facilitate a realistic assessment of the short- and long-term impacts of ocean de-oxygenation and changing productivity on N-cycling in OMZs, as well as their effects on neighbouring water masses.

Materials & Methods

Physico-chemical and N-cycling rate measurements

Large-scale distributions of chemical and biological variables were determined during the cruises M77-3 and 4 from December 2008 to February 2009 onboard R/V Meteor. Seawater was collected with either a conductivity-temperature-depth (CTD) rosette system fitted with 10-L Niskin bottles or a pump-CTD system (depth range: ~375 m). Continuous vertical profiles of chlorophyll-*a* were obtained fluorometrically and calibrated against discrete values derived from acetone extraction. Oxygen was measured with a Seabird sensor, a conventional amperometric microsensor and a highly sensitive STOX (Switchable Trace amount Oxygen) sensor[39] (detection limit: 50 nmol L^{-1}). Dissolved inorganic N and PO_4^{3-} concentrations were analyzed using standard protocols[45,46]. Nitrogen deficits were calculated as N* following Gruber & Sarmiento[47]. Rates of microbial N-cycling (NH_3 and NO_2^- oxidation, NO_3^- reduction, anammox, denitrification and DNRA) were determined in short-term, time-series incubation experiments with various combinations of ^{15}N-labeled and unlabelled compounds as described in Füssel et al.[22] and Holtapples et al.[48]. Oxygen sensitivity assays for NO_2^- oxidation were conducted as previously described[22]. Consistent rates for anammox were calculated from the various ^{15}N-incubation experiments

($^{15}NH_4^+ \pm {}^{14}NO_2^-$, $^{15}NO_2^- \pm {}^{14}NH_4^+$, $^{15}NO_2^- \pm {}^{14}NH_4^+$) for coastal OMZ stations; whereas more variability was associated with offshore OMZ stations. Although the possibility of substrate stimulation due to $^{15}N/^{14}N$-amendments cannot be fully eliminated, marine microbes including anammox and nitrifying bacteria[13,22] are often associated with particles, and thus can experience substrate concentrations several orders of magnitude greater than the ambient water[49] such that our measured rates could also be substantially underestimated. In order to examine whether the export production is sufficient to support these measured rates of various subsurface N-cycling processes and ultimately N-loss, the maximum potential rates for anammox from the various isotope-amendments (Supplementary Table 2) were used in budget calculations. Based on our combined rate measurements, nutrient inventories and subsequent modeling, the N-fluxes are sufficient to support all measured rates of N transformation. Hence, the here-presented measured rates may not be too far from reality.

Molecular ecological analyses

Water samples for nucleic-acids-based analyses were collected onto polyethersulfone membrane filters (0.2 μm; Millipore) and immediately frozen at -80°C until further analysis. Nucleic acids were extracted using a Qiagen DNA/RNA All prep Kit following the manufacturers protocol with minor modifications[50]. Functional genes for archaeal and bacterial (β-/γ-proteobacterial) NH_3 oxidation (arch-*amoA* and β-/γ-*amo*A, respectively), anammox (*hzo*1 and 2), denitrification (denitrifier-*nirS*) and DNRA (*nrfA*) were PCR-amplified as described in Löscher et al.[49]. Standards for quantitative PCRs were obtained from: *Nitrosococcus oceani* NC10 and *Nitrosomonas marina* NM22 and NM51 (γ- and β-*amoA*, respectively), an environmental clone (GenBank accession number JF796147; arch-amoA), *Candidatus* "Scalindua profunda" (hzo1 and 2), *Pseudomonas aeruginosa* PAO1 (denitrifier-*nirS*) and *Escherichia coli* K12 (*nrfA*).

Modeling of export production

Export production was calculated from estimates of net primary production and the ratio of export production to total primary production (*ef*-ratio). Net primary production (NPP) at the time and location of our experimental stations was computed from measured chlorophyll-a concentrations and satellite-based (MODIS ocean color data) estimates of photosynthetic available radiation using the Vertically Generalized Production model[42]. *Ef*-ratios were calculated from NPP and measured surface temperatures after Laws et al.[43].

Author contributions

TK, GL and MK designed the study. TK, GL, SC and AP performed ^{15}N-labeling experiments. TK, GL and PL analyzed the data. CL carried out functional gene analyses. LA and AO modelled export production rates. LS provided CTD and ADCP data. TK, GL, PL and MK wrote the manuscript.

The authors declare no competing financial interests.

References

1. Kamykowski, D. & Zentara, S. Hypoxia in the world ocean as recorded in the historical data set. *Deep-Sea Res.* **37**, 1861-1874 (1990).
2. Karstensen, J., Stramma, L. & Visbeck, M. Oxygen minimum zones in the eastern tropical Atlantic and Pacific oceans. *Progr. Oceanogr.* **77**, 331-350 (2008).

3. Diaz, R.J. & Rosenberg, R. Spreading Dead Zones and Consequences for Marine Ecosystems. *Science* **321**, 926-929 (2008).

4. Stramma, L. et al. Expanding Oxygen-Minimum Zones in the Tropical Oceans. *Science* **320**, 655-658 (2008).

5. Keeling, R.F., Körtzinger, A. & Gruber, N. Ocean Deoxygenation in a Warming World. *Ann. Rev. Mar. Sci.* 463-493 (2009).

6. Lam, P. & Kuypers, M.M. Microbial Nitrogen Cycling Processes in Oxygen Minimum Zones. *Ann. Rev. Mar. Sci.* **3**, 317-347 (2011).

7. Gruber, N. The Dynamics of the Marine Nitrogen Cycle and its Influence on Atmospheric CO2. *NATO ASI Series* 97-148 (2004).

8. Deutsch, C. et al. Climate-Forced Variability of Ocean Hypoxia. *Science* **333**, 336-339 (2011).

9. Moore, J.K. & Doney, S.C. Iron availability limits the ocean nitrogen inventory stabilizing feedbacks between marine denitrification and nitrogen fixation. *Glob. Biogeochem. Cyc.* **21**, GB2001 (2007).

10. Schmittner, A. et al. Future changes in climate, ocean circulation, ecosystems, and biogeochemical cycling simulated for a business-as-usual CO2 emission scenario until year 4000 AD. *Glob. Biogeochem. Cyc.* **22**, GB1013 (2008).

11. Somes, C.J. et al. Simulating the global distribution of nitrogen isotopes in the ocean. *Glob. Biogeochem. Cyc.* **24**, GB4019 (2010).

12. Kuypers, M.M. et al. Massive nitrogen loss from the Benguela upwelling system through anaerobic ammonium oxidation. *PNAS* **102**, 6478-6483 (2005).

13. Hamersley, M.R. et al. Anaerobic ammonium oxidation in the Peruvian oxygen minimum zone. *Limnol. Oceanogr.* **52**, 923-933 (2007).

14. Jensen, M.M. et al. Intensive nitrogen loss over the Omani Shelf due to anammox coupled with dissimilatory nitrite reduction to ammonium. *ISME* **AOP** (2011).

15. Lam, P. et al. Origin and fate of the secondary nitrite maximum in the Arabian Sea. *Biogeosciences* **8**, 1565-1577 (2011).

16. Bohlen, L. et al. Benthic nitrogen cycling traversing the Peruvian oxygen minimum zone. *Geoch. Cosmoch. Acta* **75**, 6094-6111 (2011).

17. Cline, J.D. & Richards, F.A. Oxygen Deficient Conditions and Nitrate Reduction in the Eastern Tropical North Pacific Ocean. *Limnol. Oceanogr.* **17**, 885-900 (1972).

18. Codispoti, L.A. & Packard, T.T. Denitrification Rates in the Eastern Tropical South-Pacific. *J. Mar. Res.* **38**, 453-477 (1980).

19. Naqvi, S.W. Some aspects of the oxygen-deficient conditions and denitrification in the Arabian Sea. *J. Mar. Res.* **45**, 1049-1072 (1987).

20. Thamdrup, B. et al. Anaerobic ammonium oxidation in the oxygen-deficient waters off northern Chile. *Limnol. Oceanogr.* **51**, 2145-2156 (2006).

21. Lam, P. et al. Revising the nitrogen cycle in the Peruvian oxygen minimum zone. *PNAS* **106**, 4752-4757 (2009).

22. Füssel, J. et al. Nitrite oxidation in the Namibian oxygen minimum zone. *ISME* **AOP** (2011).

23. Lipschultz, F. et al. Bacterial transformations of inorganic nitrogen in the oxygen-deficient waters of the Eastern Tropical South Pacific Ocean. *Deep-Sea Res.* **37**, 1513-1541 (1990).

24. Kalvelage, T. et al. Oxygen Sensitivity of Anammox and Coupled N-Cycle Processes in Oxygen Minimum Zones. *PLoS ONE* **6**, e29299 (2011).

25. Fuenzalida, R. et al. Vertical and horizontal extension of the oxygen minimum zone in the eastern South Pacific Ocean. *Deep-Sea Res. II* **56**, 992-1003 (2009).

26. Codispoti, L.A. & Christensen, J.P. Nitrification, Denitrification and Nitrous Oxide Cycling in the Eastern Tropical South Pacific Ocean. *Marine Chemistry* **16**, 277-300 (1985).

27. Wooster, W.S., Chow, T.J. & Barrett, I. Nitrite Distribution in Peru Current Waters. *J. Mar. Res.* **23**, 210-221 (1965).

28. Nelson, S.S. & Neshyba, S. On the southernmost extension of the Peru-Chile Undercurrent. *Deep-Sea Res.* **26A**, 1387-1393 (1979).

29. Ward, B.B., Glover, H.E. & Lipschultz, F. Chemoautotrophic Activity and Nitrification in the Oxygen Minimum Zone off Peru. *Deep-Sea Res.* **36**, 1031-1051 (1989).

30. Fernández, C., Farías, L. & Alcaman, M.E. Primary production and nitrogen regeneration processes in surface waters of the Peruvian upwelling system. *Progr. Oceanogr.* **83**, 159-168 (2009).

31. Anderson, J.J. et al. A model for nitrite and nitrate distributions in oceanic oxygen minimum zones. *Deep-Sea Res.* **29**, 1113-1140 (1982).

32. Lavik, G. et al. Detoxification of sulphidic African shelf waters by blooming chemolithotrophs. *Nature* **457**, 581-584 (2008).

33. Dalsgaard, T. et al. Anammox and denitrification in the oxygen minimum zone of the eastern South Pacific. *Limnol. Oceanogr.* **57**, 1331-1346 (2012).

34. Ward, B.B. et al. Denitrification as the dominant nitrogen loss process in the Arabian Sea. *Nature* **461**, 78-81 (2009).

35. Deutsch, C. et al. Denitrification and N2 Fixation in the Pacific Ocean. *Glob. Biogeochem. Cyc.* **15**, 483-506 (2001).

36. Dalsgaard, T. et al. N2 production by the anammox reaction in the anoxic water column of Golfo Dulce, Costa Rica. *Nature* **422**, 606-608 (2003).

37. Van Mooy, B.A., Keil, R.G. & Devol, A.H. Impact of suboxia on sinking particulate organic carbon: Enhanced carbon flux and preferential degradation of amino acids via denitrification. *Geoch. Cosmoch. Acta* **66**, 457- 465 (2002).

38. Canfield, D.E. et al. A Cryptic Sulfur Cycle in Oxygen-Minimum Zone Waters off the Chilean Coast. *Science* **330**, 1375-1378 (2010).

39. Revsbech, N.P. et al. Determination of ultra-low oxygen concentrations in oxygen minimum zones by the STOX sensor. *Limnol. Oceanogr.: Methods* **7**, 371-381 (2009).

40. Thamdrup, B., Dalsgaard, T. & Revsbech, N.P. Widespread functional anoxia in the oxygen minimum zone of the eastern South Pacific. *Deep-Sea Res. I* in Press (2012).

41. Bertrand, A., Ballón, M. & Chaigneau, A. Acoustic Observation of Living Organisms Reveals the Upper Limit of the Oxygen Minimum Zone. *PLoS ONE* **5**, e10330 (2010).

42. Behrenfeld, M.J. & Falkowski, P.G. Photosynthetic rates derived from satellite-based chlorophyll concentration. *Limnol. Oceanogr.* **42**, 1-20 (1997).

43. Laws, E.A. et al. Temperature effects on export production in the open ocean. *Glob. Biogeochem. Cyc.* **14**, 1231-1246 (2000).

44. Pennington, J.T. et al. Primary production in the eastern tropical Pacific: A review. *Progr. Oceanogr.* **69**, 285-317 (2006).

45. Grasshoff, K. et al. *Methods of seawater analysis*. (Wiley: 1999).

46. Holmes, R.M. et al. A simple and precise method for measuring ammonium in marine and freshwater ecosystems. *Canadian Journal of Fisheries and Aquatic Sciences* **56**, 1801-1808 (1999).

47. Gruber, N. & Sarmiento, J.L. Global Patterns of Marine Nitrogen Fixation and Denitrification. *Glob. Biogeochem. Cyc.* **11**, 235-266 (1997).

48. Holtappels, M. et al. 15N-labeling experiments to dissect the contributions of heterotrophic denitrification and anammox to nitrogen removal in the OMZ waters of the ocean. *Methods Enzymol.* **486**, 223-251 (2011).

49. Stocker, R. Marine Microbes See a Sea of Gradients. *Science* **338**, 628-633 (2012).

50. Loescher, C.R. et al. Production of oceanic nitrous oxide by ammonia-oxidizing archaea. *Biogeosc. Disc.* **9**, 2095-2122 (2012).

Correspondence and requests for materials should be directed to: mkuypers@mpi-bremen.de

455

Acknowledgements

We wish to thank the Peruvian government for access to their territorial waters. We sincerely thank cruise leader Martin Frank as well as the crews of the cruises M77-3 and 4 onboard *R/V Meteor* for their support at sea. We are grateful for the technical and analytical assistance of Gabriele Klockgether, Inka Boosmann, Violeta Leon, Imke Grefe and Andreas Ellrott. We thank Niels Peter Revsbech, who generously provided the STOX sensors and Tim Ferdelmann for offering valuable comments to improve the article. This study was supported by the Deutsche Forschungsgemeinschaft through the Sonderforschungsbereich 754 "Climate-Biogeochemistry Interactions in the Tropical Ocean" and the Max Planck Society.

460

465

Table 1 | Abundance of selected N-functional genes and N-conversion rates in the ETSP during cruise M77-3.

Functional genes and N-conversion rates were not always determined at the same station and/or depths but with a comparable latitudinal and longitudinal as well as vertical resolution.

		N-functional gene abundances (10^2 copies mL^{-1})							N-conversion rates (nmol N L^{-1} d^{-1})					
		arch-amoA	β-amoA	γ-amoA	hzo1	hzo2	den-nirS*	nrfA	NH_3 ox.	Anammox	Denitri-fication	DNRA	NO_2^- ox.	NO_3^- red.
Coastal OMZ (≤600 m)	N:	63 (64)	8 (49)	0 (64)	8 (64)	42 (64)	0 (63)	0 (64)	27 (33)	33 (33)	3 (33)	7 (33)	27 (32)	27 (32)
	Range:	0.16-2773	0.05-1056	-	0.05-0.09	0.14-12.8	-	-	0.22-48.8	2.84-227	2.21-5.42	0.48-1.74	8.48-928	3.79-1010
	Mean:	676	135	-	0.07	4.45	-	-	8.24	43.4	4.19	1.14	172	203
	Median:	90	5.0	-	0.06	3.77	-	-	3.40	21.2	4.94	1.10	65.4	101
Offshore OMZ (>600 m)	N:	67 (71)	2 (33)	0 (72)	4 (71)	43 (72)	2 (72)	1 (72)	17 (40)	33 (40)	0 (40)	3 (40)	27 (40)	25 (34)
	Range:	0.04-2332	0.15-1.36	-	0.01-0.09	0.06-14.7	0.06-1.98	0.11	0.51-88.8	0.71-46.9	-	0.33-1.31	4.58-186	4.53-77.4
	Mean:	352	0.75	-	0.08	3.15	1.02	0.11	20.9	6.14	-	0.82	40.6	32.1
	Median:	89.5	0.75	-	0.08	1.51	1.02	0.11	5.79	3.01	-	0.83	30.2	22.3

N = number of samples in which N-functional genes/N-processes were detected; in parenthesis: number of samples analyzed.
*denitrifier-nirS.

Table 2 | Spearman rank correlation of depth-integrated nutrients and N-cycling rates as well as modelled export productions.

	NH_3 oxidation	NO_2^- oxidation	NO_3^- reduction	Anammox	Export Production
NH_4^+	0.51*	0.31	0.08	0.30	0.29
NO_2^-	0.46*	0.49*	0.71***	0.64**	0.10
N*	-0.08	-0.20	-0.05	-0.02	-0.02
Export Production	0.56*	0.60**	0.75***	0.79***	
Anammox	0.75***	0.86***	0.88***		
NO_3^- reduction	0.49*	0.75***			
NO_2^- oxidation	0.73***				

Presented values are correlation coefficients with significant values denoted by * ($p \leq 0.05$), ** ($p \leq 0.01$) and *** ($p \leq 0.001$).

Figure legends

Figure 1 | Maps of sampling locations and nutrient distributions in the ETSP OMZ. a, Sampling sites during M77-3 (●) and M77-4 (●) and ^{15}N-experimental stations (●). **b**, vertical extent of the OMZ (in m) as defined by $O_2 \leq 15$ µmol L^{-1}. **c-f**, concentrations of NO_3^-, NO_2^-, NH_4^+ and N* (in mol m^{-2}) integrated over the thickness of the OMZ. Red line in panel **a**. denotes the 600m-isobath that was used demarcate the coastal OMZ from offshore OMZ.

Figure 2 | Depth-integrated N-cycling rates in the ETSP OMZ. a,**b**, the two steps of the aerobic nitrification, NH_3 oxidation and NO_2^- oxidation. **c**, NO_3^- reduction to NO_2^-. **d**,**e**, N-loss due to anammox as well as denitrification coupled to the oxidation of H_2S during a sulfidic event on the Peruvian shelf. **f**, modelled export of organic N from the euphotic zone to the OMZ. All rates in mmol N m^{-2} d^{-1}.

Figure 3 | N-fluxes and nutrient inventory of the ETSP OMZ. Black numbers indicate inventories of dissolved inorganic nitrogen (in Tg N). They were derived from the depth-integrated values over the OMZ thickness shown in Figs. 1-2, and then based on the 600 m seafloor depth cut-off for coastal versus offshore OMZs, the depth-integrated values were further integrated over the areal extents of the two types of OMZs. Fluxes (in Tg N y^{-1}) within the OMZ or across its boundaries are given in colour and white, respectively. A detailed description of the flux calculations is included in the supplementary information.

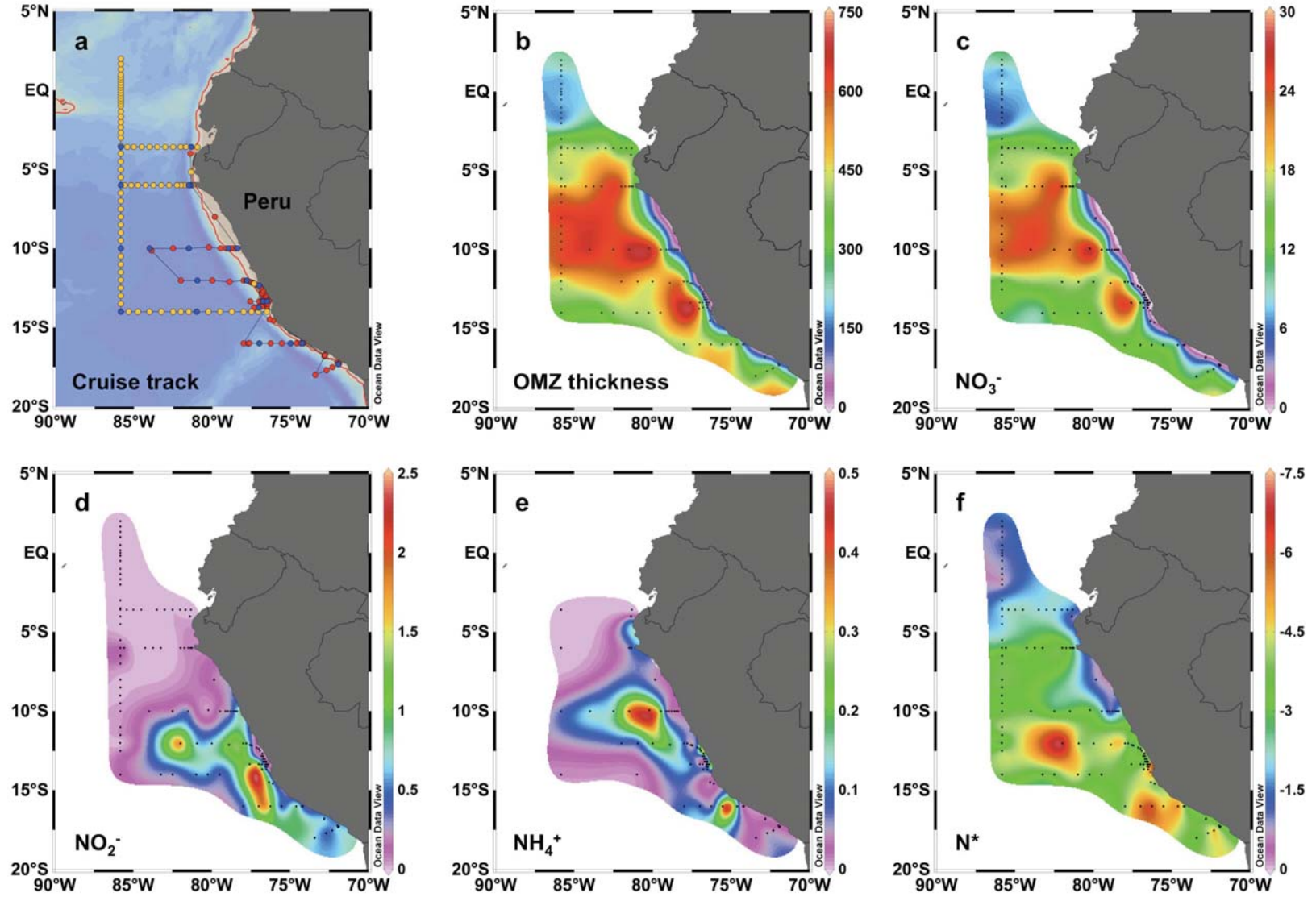
a
Peru
Cruise track
b
OMZ thickness
c
NO_3^-
d
NO_2^-
e
NH_4^+
f
N*
5°N
EQ
5°S
10°S
15°S
20°S
90°W
85°W
80°W
75°W
70°W
Ocean Data View
750
600
450
300
150
0
30
24
18
12
6
0
2.5
2
1.5
1
0.5
0
0.5
0.4
0.3
0.2
0.1
0
-7.5
-6
-4.5
-3
-1.5
0

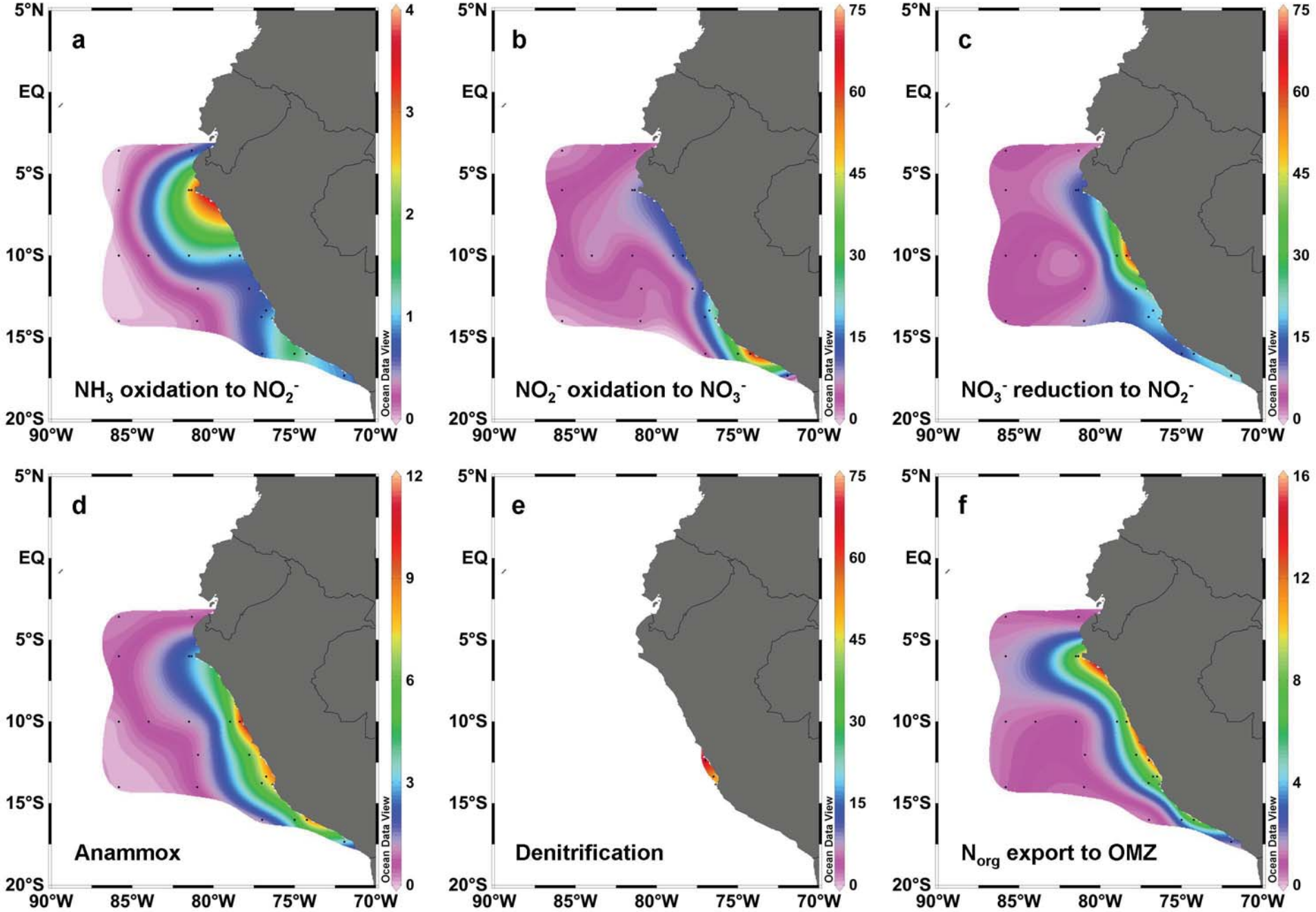
a
NH_3 oxidation to NO_2^-
b
NO_2^- oxidation to NO_3^-
c
NO_3^- reduction to NO_2^-
d
Anammox
e
Denitrification
f
N_{org} export to OMZ
5°N
EQ
5°S
10°S
15°S
20°S
90°W
85°W
80°W
75°W
70°W
Ocean Data View
0
1
2
3
4
15
30
45
60
75
6
9
12
8
16

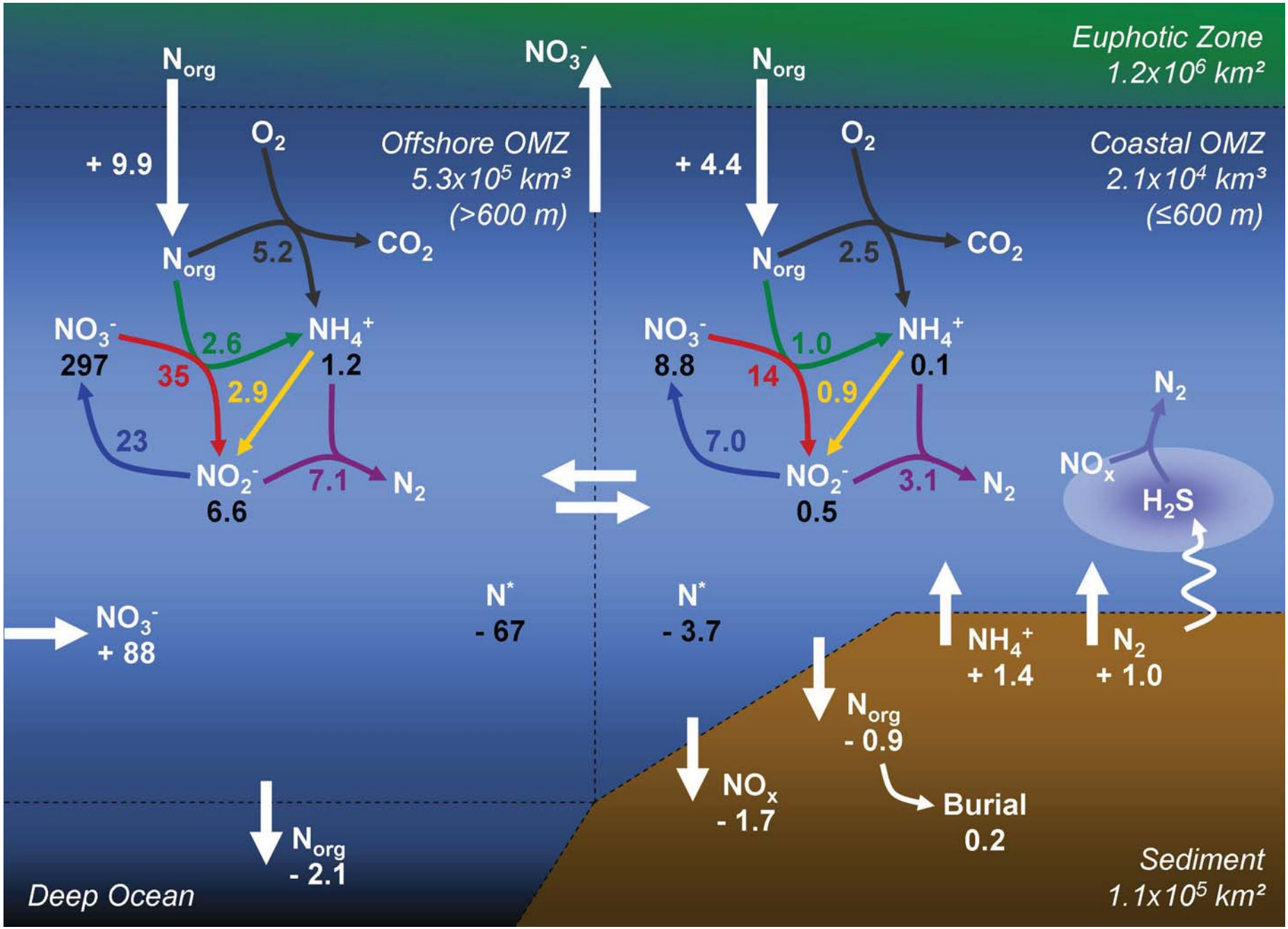
Euphotic Zone
1.2x10⁶ km²
Offshore OMZ
5.3x10⁵ km³
(>600 m)
Coastal OMZ
2.1x10⁴ km³
(≤600 m)
Norg
+ 9.9
O2
CO2
5.2
NO3-
297
2.6
NH4+
1.2
35
2.9
23
NO2-
6.6
7.1
N2
+ 4.4
2.5
8.8
1.0
0.1
14
0.9
7.0
0.5
3.1
NOx
H2S
NO3-
+ 88
N*
- 67
N*
- 3.7
NH4+
+ 1.4
N2
+ 1.0
Norg
- 0.9
NOx
- 1.7
Burial
0.2
Norg
- 2.1
Deep Ocean
Sediment
1.1x10⁵ km²